CFD Optimization of Transonic Low Pressure Turbine Blade

Firat Kiyici[1], Tolga Yasa[2], Emiliano Costa[3] and Stefano Porziani[3]

[1]Tusas Engine Industry, Eskisehir, Turkey
[2]Anadolu University, Eskisehir, Turkey
[2]D'Appolonia SpA, Rome, Italy

Corresponding author: firat.kiyici@tei.com.tr

Abstract: Performance of a transonic low pressure turbine blade is investigated by using Radial Basis Functions (RBF) mesh morphing. The drag coefficient is defined as airfoil performance parameter. The drag coefficient of airfoil is computed using three dimensional Reynolds Averaged Navier Stokes (RANS) solver with hybrid grid topology. Laminar model, k-ω SST and k-ω Transition SST turbulence models are studied on the baseline blade configuration to investigate transition location and flow separation. Drag coefficient is reduced by 4.5% with RBF4AERO optimization tool.

Keywords: Transonic Turbine, Radial Basis Functions, Computational Fluid Dynamics, Turbulence Modeling, Mesh Morphing

1   Introduction

The low pressure turbine (LPT) stage is one of the heavy structures of aero-engines. Therefore, substantial effort has been spend to reduce the weight of the component. The main effort of weight reduction has been focused on the reduction of number of airfoil since the LPT stages have high solidity. Moreover, such reduction is also beneficial since it reduces the cost of the component. The flow around the LPT blades is within the critical Reynolds number range. Hence, laminar to turbulence transition occurs when the flow passing around the airfoil. LPT has the lowest Reynolds number compared to the other turbine types in aero engines. So, development of the boundary layer is occurred by transition from laminar flow regime to turbulent. Such transition is critical because it may cause flow separation and reduction of power.

Aerodynamic loss is the (or one of the) main problem in turbomachinery and it is measured by entropy generation [1]. Entropy generation occurs because of viscous dissipation, temperature differences and non-equilibrium processes such as shock waves. Viscous dissipation in the blade surface boundary layers is the main source of loss in LP turbines [2-5]. Effects of Mach and Reynolds number on loss production are investigated in Vazguez et. al [6,7]. According to these studies, increasing Mach numbers, maximum velocity that occurs on the suction side moves downstream and it leads to increase in adverse pressure gradients. These gradients cause flow separation of boundary layer and generate shock waves. Furthermore, for higher flow speed, the blade shock system interacts with the adjacent airfoils and may cause sudden loss rises and shock induced flow separation [8]. Shock induced flow separations are widely investigated both experimentally and numerically [9-13].

Blade optimization studies are widely investigated by researchers. In Ellbrant's study [14] transonic compressor blade optimization was performed with using multi-objective functions with metamodels such as Neural Networks Kriging and RBF. According to the study, RBF is faster and more effective than the other metamodels and it reduces to convergence time two weeks to 3.5 days. Moshizi et al. [15] compare VKI's gas turbines blade cascade's inviscid and viscous transonic flow field. The study shows that viscous and inviscid solutions give similar results and there is an agreement with both numerical and Emery's et al. experimental results [16]. Moreover, 2D and 3D numerical optimization

studies are performed to reduce shock wave effects [17-19].

Even though spring analogy is used commonly for mesh deformation, it has some limitations. So, innovative methods are developed to overcome the spring analogy problems. One of the crucial important deformation techniques is RBF. RBF is very practical to use with unstructured grids it provides high robustness [20]. Main advantage of the RBF based deformation is moving grid points and interpolating the displacements independently. In turbomachinery, RBF method is getting popular and it is used in design and optimization process [21-23]. RBF4AERO is an EU funded project to develop innovative optimization tool based on mesh morphing. Main advantage of the platform is to reduce computational time to find optimal solution with metamodel assisted evolutionary algorithms. Also, RBF4AERO has a meshless approach and it is also efficient than other shape parameterization techniques. Commonly, shape parameterization techniques use surface grid points to be deformed with costly remeshing process. To overcome the problem, in RBF method, grid points are moved in user defined area regardless their connectivity and displacements of grid points could be defined by user.

In this study, a transonic LPT blade is optimized with RBF4AERO platform to enhance the airfoil performance in terms of drag coefficient.

2 Turbine Blade Model and Numerical Setup

The model airfoil is designed for a demonstrator LPT airfoil which aims to operate at transonic speed at design conditions. The model airfoil parameters are given in Table1. The performance of the airfoil is investigated numerically by solving two dimensional RANS equations.

Table 1. Airfoil Geometry Properties

Rotor Foil Parameters	Value
Axial Chord (C_{ax})	18.03 mm
Pitch/Chord Ratio	0.72
Total Turning Angle	15.5 deg.
M_{2is}	1
Re	90000 – 110000
Stage Loading, $\Delta H/U^2$	1.4

The numerical simulations are performed by using commercial software Ansys-Fluent. Solution domain is discretized into a hybrid mesh using finite volume approach and is iteratively solved for each of velocity, pressure, density and temperature subjected to stability, and consistency consideration. The numerical computation is performed by applying finite volume principle on the governing conservation equation of mass, momentum and energy equations subjected to inlet (total conditions: velocity, turbulence, temperature) outlet (zero gradient pressure and turbulence) and surface no slip (zero velocity) boundary conditions. These equations are solved in a sequence using an iterative scheme. The convective fluxes are discretized using 2nd order upwind scheme and the diffusion term following a centralized 2nd order scheme. The convergence is achieved when value of scaled residuals of continuity, energy and momentum equation reached as low as 10-E6. Also, control points are created pressure and suction sides of the airfoil to check the convergence in terms of drag and lift coefficient values

With the principal purposes to detect whether a shock and the separation of boundary layer occur in steady state working conditions reproducing those characterizing the wind tunnel testing, the 2D aerodynamic analyses of the LPT design mean line profile are conducted for both fully laminar and fully turbulent flow conditions. In specific, the study with the fully laminar model basically aimed at generating the outputs to be compared with the ones gained through the fully turbulence models to differentiate the turbulence contribution. Referring to turbulence models, the k-ω SST and transition SST models are selected as they are the most reliable and accurate in simulating low-Re turbulent flows in the turbine stage as well as in detecting the separation of turbulent boundary layers.

The k-ω SST is based on the use of transport equations for turbulent kinetic energy k and rate of dissipation ω, whilst the transition SST is based on the coupling of the k-ω SST transport equations with two other transport equations, one for the intermittency and one for the transition onset criteria. The Intermittency parameter, in particular, is a measure of the probability that a given point is located

inside a turbulent region. Given that, upstream of transition the intermittency is zero and, once the transition occurs, the intermittency is ramped up to one until the fully turbulent boundary layer regime is achieved.

The numerical domain consists of one 2D blade geometry. Typical mesh is depicted in Figure 2. The structured mesh is preferred around the airfoil in the boundary layer section whereas unstructured topology is selected for the rest of the domain. Inlet section of the domain has a length of $0.7*C_{ax}$ while the domain outlet is fixed $0.7*C_{ax}$ downstream of the airfoil trailing edge in order to prevent any numerical reflection from outlet. The mesh dependency analysis is performed for three mesh configurations as listed in Table 2. Wall y^+ values are kept lower than 1.

Table 2. Mesh Properties

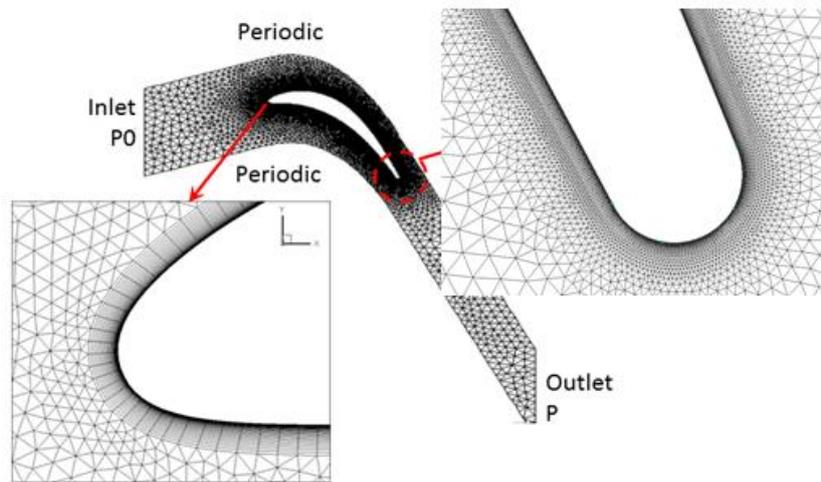| Mesh Type	Number of Grid Points
Coarse	100000
Medium	420000
Fine	1760000

Figure 1. Mesh topology of the numerical domain

The total pressure is defined at the inlet of the domain while the static pressure is used at the outlet to establish the desired flow at the domain. The periodic flow condition is used for the lateral boundaries to simulate airfoil cascade.

The simulation is performed for three types of flow conditions. In the first assumption, the flow is assumed to be fully turbulent and the turbulence is modelled by using k-ω SST [24]. The k-ω SST is based on the use of transport equations for turbulent kinetic energy k and rate of dissipation ω. For the second solver setup the transition criteria developed by Menter [25] is added to the fully turbulent configuration. The second case (SST with transition) is based on the coupling of the k-ω SST transport equations with two other transport equations, one for the intermittency and one for the transition onset criteria which is formulated by. In the final approach, the incoming flow is assumed to be laminar. Hence, the laminar to turbulent transition occurs by the nature of the flow.

4 Optimization Methodology

The performance of baseline model is enhanced by optimization. Airfoils are generated through mesh morphing and the Evolutionary Algorithms (EAs) based tool assisted by metamodels trained on a sampling performed during the Design of Experiment (DoE) phase is used along with a CFD evaluation tool with the use of Response Surface Models (RSM) the significantly reduces the number of CFD runs required to reach the optimal solution. First, the baseline airfoil is geometrically modified to generate a design space for optimization. Design of Experiment (DoE) technique is used to select proper samples from the design space. Then, numerical simulations are performed on the selected samples to evaluate airfoil performance of the candidates. An optimization database is generated from those results and it is used to train the RSM. Finally, RSM is evaluated for

an optimum airfoil. Numerical simulation is also performed on the optimum geometry. The result of simulation performed with optimum airfoil is also added to the optimization database. RSM is again trained by using updated database and new meta-model is evaluated for a second time for an optimum airfoil. This process is continued until the geometry of the optimum airfoil is converged. The process chart of the optimization process is depicted in Figure 3.
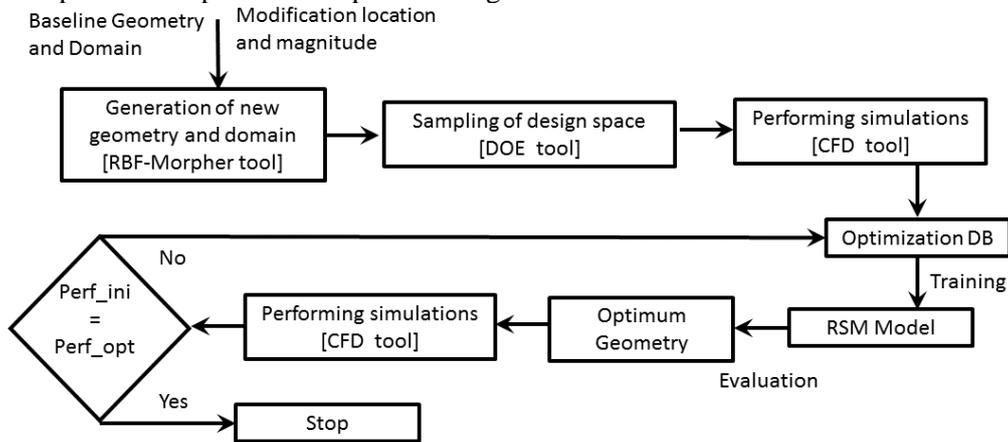

Figure 3. Algorithm of the RBF4AERO optimization process

The numerical setup by means of mesh topology and flow settings of baseline configuration is respected for all simulations during the optimization process. Once the airfoil is geometrically modified, the initial mesh topology is morphed accordingly using RBF. Highly skewed elements and negative volumes are not allowed by the morpher tool during such modifications. This technique does not require any re-meshing operation therefore it is practical and time-saving. The whole optimization process is controlled by an optimization manager and automatized in a special tool [26] that is developed under an EU FP7 project called RBF4AERO. User only decides the location and the magnitude of the modification

3   Flow Field Analysis of Baseline Model

Isentropic Mach number distribution is plotted in Figure 3 for the three mesh configuration. Flow suddenly accelerates at the front part of the airfoil due to the high leading edge curvature. Then, flow accelerates smoothly up to the throat and trailing edge of the airfoil at the suction side and pressure side, respectively. At the throat, the Isentropic Mach number (M_{is},) reaches its maximum level of 1.18. At the throat region, the trailing edge shock of the adjacent airfoil impinges on the suction side causing a sudden reduction of M_{is}. Downstream of the impingement location flow decelerates smoothly until the trailing edge. All mesh configurations result in similar M_{is} distributions. The coarse mesh configuration is slightly over estimate M_{is} at the impingement location. Hence, coarse mesh configuration is used for optimization study in order to reduce computational cost.
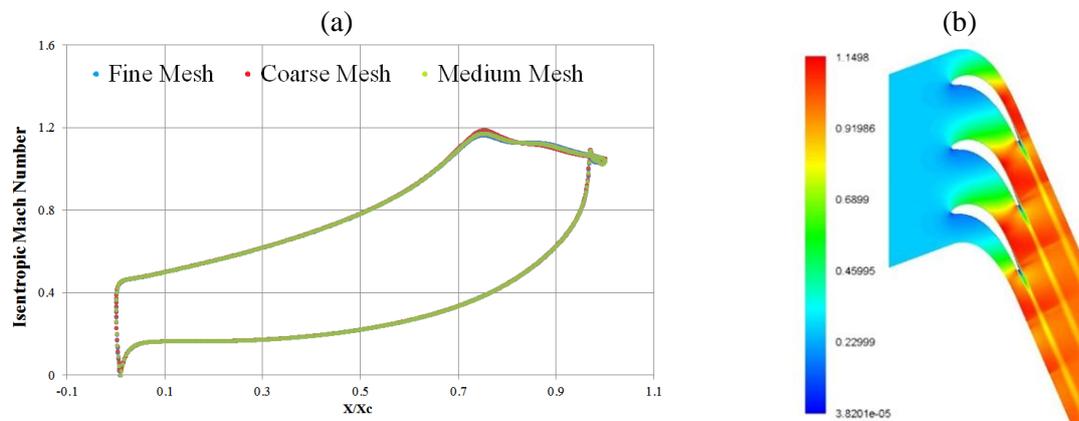

Figure 4. Isentropic Mach Number a) around the airfoil b) blade to blade contour

Turbulence model comparison study is also performed. It is crucial to define the transition location for

an LPT airfoil since the performance is directly linked with the boundary layer status and its behavior after the laminar to turbulent transition. In Figure 5, Results from three different solver configurations using k-ω SST turbulence models with transition, k-ω SST turbulence models and laminar model are compared at 5% turbulence intensity. The shock impingement location moves downstream when k-ω SST turbulence model with transition and laminar model are used. Hence, the maximum M_{is} reached at the throat region is greater when those two models are employed. The transition location is investigated by studying skin friction distribution depicted in Figure 5-B. It is distinguished by the sudden reduction of the skin friction coefficient. Based on Figure 5-B the starting location of transition is similar for all three models. However, boundary layer becomes turbulent rapidly when SST model is used while it needs more distance for the other two models. k-ω SST turbulence model with transition is selected as a proper solver configuration in the optimization study.
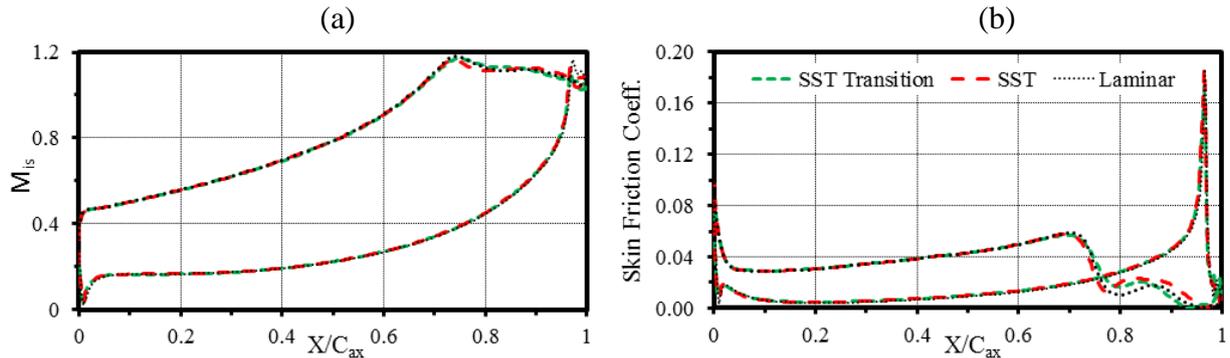

Figure 5. Effect of flow parameter on a) Isentropic Mach Number b) Skin Friction Distribution

The turbulence intensity is a crucial parameter for the transition onset therefore the effect of turbulence intensity on the boundary layer characteristics are studied for three different turbulence intensities namely, low (0.6%), medium (2%) and high (5%). Figure 6 shows M_{is} and skin friction coefficient distribution of the airfoil at design conditions for three turbulence intensity levels. When the turbulence intensity of the main stream is increased, the onset of transition moves upstream. Moreover, it turns to turbulent state more quickly than low level of turbulence.
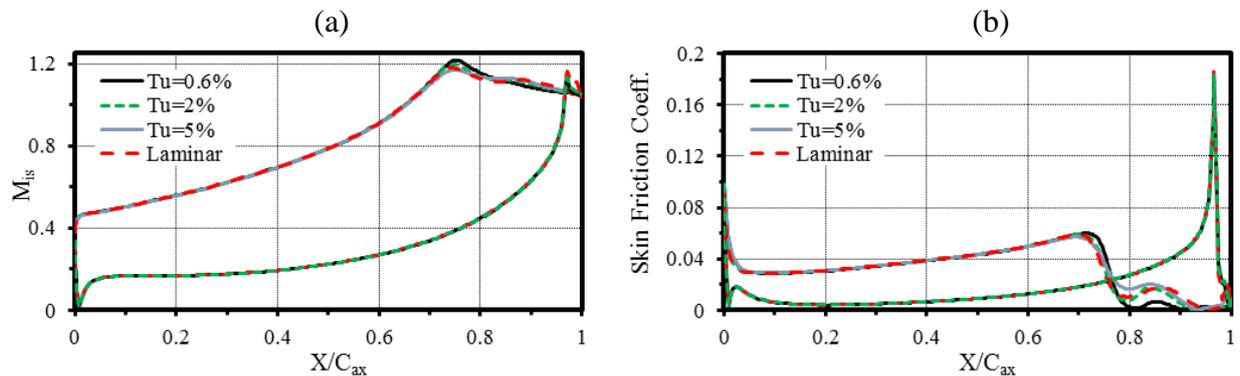

Figure 6. Effect of turbulence intensity a) Isentropic Mach Number b) Skin Friction Distribution

4   Optimization Results

The optimization process of LPT airfoil is focused on the rear geometry as shown in Fig.7-A. The main aim of the process is to reduce aerodynamic loss while keeping the lift coefficient of the geometry at the same level. The drag coefficient is used as a performance parameter during the process. The geometrical modifications at the selected section in limited as depicted in Fig.7-B. Small morphing displacements are defined due to the transonic characteristics of the flow this region is extremely sensitive to any displacement applied.
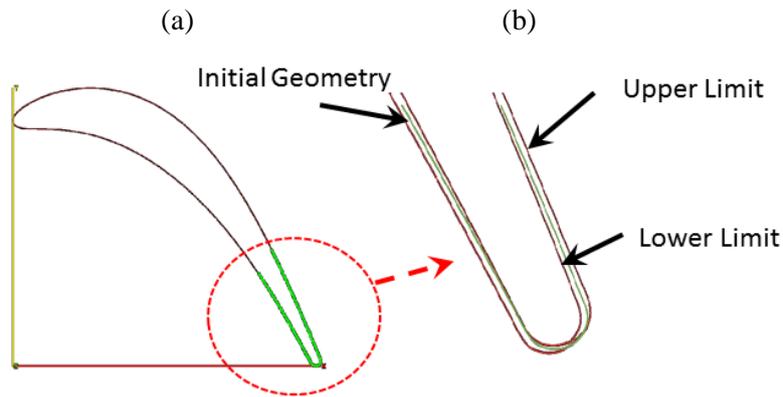
Figure 7. A) Source Points for Shape Deformation B) Upper and Lower Deformation Limits

The evaluation of drag coefficient is presented in Fig.8-A. Two design variables are defined to deform pressure and suction side of the LPT blade at the trailing edge section. Design space was created with 33 samples. They are used to train a fourth order RSM. Evolutionary algorithm is employed for the optimization with a termination criterion of 250 evaluations on the RSM and 9 iterative cycles are defined to meet convergence criteria. Drag coefficient is reduced approximately 4.5% of the baseline one for the final geometry. Initial and optimized geometries are also compared in Fig.8-B.
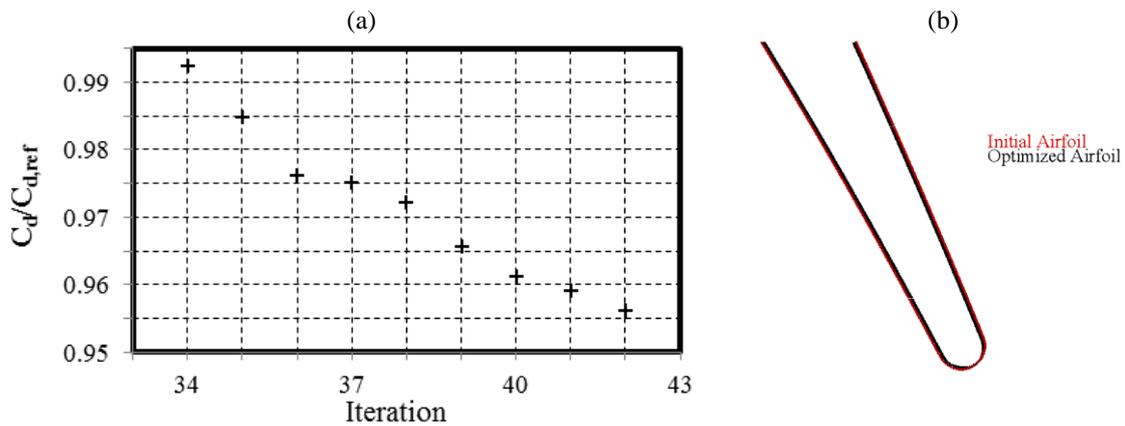

Figure 8. Comparision of initial and optimized airfoils a) Drag Coefficient Evolution b) Geometries

Performances of both airfoils are compared in Figure 9 in terms of M_{is} and skin friction distributions. The optimized airfoil results in more smooth deceleration downstream of the throat. The smooth deceleration also affects the boundary layer status. Although the transition onset is similar for both geometries, turbulent boundary layer starts much earlier compared to the initial case. According to Figure 9, Mach number and skin friction coefficient distribute more smoothly on the optimized blade. On the initial blade, there is a transition location at the 81% of the normalized chord but the transition also disappears on the optimized blade and thus drags coefficient decreases for optimized case.
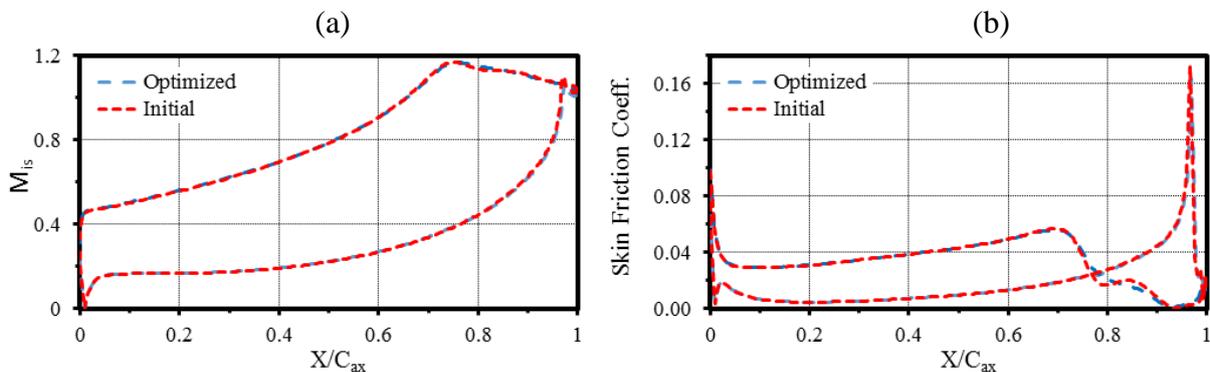

Figure 9. Comparison of A) Isentropic Mach Number B) Skin Friction Coefficient

Total computation time has taken approximately 92 hours in 32 cores Xeon processors. RBF4AERO reduces the total optimization time by 24% from adjoint-based optimization tools and gives better results in terms of airfoil performance. As a result of the RBF4AERO optimization, flow separation does not occur any optimization cases due to the sensitive mesh morphing.

6. Conclusion

The performance enhancement of a transonic low pressure turbine airfoil is carried out by using an evolutionary optimization algorithm using a polynomial Response Surface Model. Initial numerical setup is respected for all computations and the mesh is morphed by using RBF which save time in the optimization process.

Results of three different flow setups namely, k-ω SST, k-ω SST with transition and laminar models are compared. In all setups the onset of the transition is predicted at the same location whereas the starting of turbulent boundary layer varies depends on the model used. It also affects the maximum velocity reached at the throat region. The effect of turbulent intensity on the skin friction coefficient is also analyzed for the level of 0.6%, 2% and 5%. Higher turbulence intensity shorter the transition length on the airfoil.

The rear section of the airfoil is optimized to reduce the airfoil loss. The loss is expressed as drag coefficient. Thirty-three airfoil geometries is considered for the optimization. Drag coefficient reduction of 4.5% is reached by the final geometry compared to the initial shape.

Acknowledgement

References

[1] Denton, J.D., 1993,"Loss mechanisms in turbomachines", ASME Journal of Turbomachinery, Vol. 115, No. 4, pp 621-656

[2] Steiger R., The Effects of Wakes on Separating Boundary Layers in Low Pressure Turbine, Cambridge University Engineering Department, February 2002

[3] Satta F., Simoni D., Ubaldi M., Zunino P.,An Experimental Investigation of the Dissipation Mechanicsm in the Suction Side Boundarly Layer of a Turbine Blade, Journal of Thermal Science, December 2008 Volume 17, Issue 4 pp. 289-297

[4] Griffin P.C., Davies M.R.D., O'Donnell F.K., Walsh E.: The Effect of Reynolds Number, Compressibility and Free Stream Turbulence on Profile Entropy Generation Rate, ASME Paper No. GT-2002-30330, (2002).

[5] Moore J., Shaffer D.M., Moore J.G. Reynolds Stresses and Dissipation Mechanisms Downstream of a Turbine Cascade, ASME Journal of Turbomachinery, vol. 109, pp. 258-267, (1986).

[6] Vázquez R., Antoranz A., Cadrecha D., Armananzas L., The Influence of Reynolds Number, Mach Number and Incidence Effects on Production in Low Pressure Turbine, Proc ASME. 4241X; Volume 6: Turbomachinery, Parts A and B: 949-960 January 01, 2006

[7] Vázquez R., Torre D., Partida F., Armananzas L., Antoranz A., The Influence of Surface Roughness on the Profile End-Wall Losses in Low Pressure Turbine, Proc ASME. 54679; Volume 7: Turbomachinery, Parts A, B and C: 877-886 January 01, 2011

[8] Jouini, D. B. M., Sjolander, S. A., and Moustapha, S. H., 2002,"Midspan Flow-Field Measurements for Two Transonic LinearTurbine Cascades at Off-Design Conditions," ASME J.Turbomach., 124(2), pp.176-186

[9] Paniagua G., Yasa T., Loma A., Castillon L., Coton T., Unsteady Strong Shock Interactions in a Transonic Turbine: Experimental and Numerical Analysis., Journal of Propulsion and Power, Vol 24. No. 4 (2008), pp. 722-731,

[10] Johnson A.B., Rigby M.J., Oldfield M.L.G., 1989, "Unsteady Aerodynamic Phenomena in a simulated wake and shock wave passing experiment". AGARD-CP-468.

[11] Dunn M.G., Bennett W.A., Delaney R.A., Rao K.V., 1990, "Investigation of Unsteady Flow through a Transonic Turbine Stage: Comparison for Time-Averaged and Phase-Resolved Pressure Data". AIAA-90-2409.

[12] Brunner, S., Fottner, L., Schiffer, H., "Comparison of Two Highly Loaded Low Pressure Turbine Cascades under the influence of Wake-Induced Transition" ASME 2000-GT-268, 2000

[13] Coton, T., Arts, T., Lefebvre, M., Liamis, N, "Unsteady and calming effects investigation on a very high lift LPT blade" ASME GT-2002-30227, 2002.

[14] Ellbrant L., Eriksson L.E., Mårtensson, H., CFD Optimization of a Transonic Compressor Using Multiobjective GA and Metamodels, ICAS 2012

[15] S.A. Moshizi, A. Madadi and M.J. Kermani. Comparison of inviscid and viscous transonic flow field in VKI gas turbine blade cascade, Alexandria Engineering Journal 2014 53, 275-280.

[16] J.C. Emery, L.J. Herring, J.R. Erwin, A.R. Felix, Systematic Two Dimensional Cascade Tests of NACA 65-Series Compressor Blades at Low Speed, 28th International Congress of the Aeronautical Sciences.

[17] Hasenjager M., Sendhoff B., Sonoda T., Arima T., Three Dimensional Aerodynamic Optimization for an Ultra-Low Bypass Ratio Transonic Turbine Blade, ASME Turbo Expo 2005: Power for Land, Sea, and Air Volume 6: Turbo Expo 2005, Parts A and B Reno, Nevada, USA, June 6–9, 2005

[18] Arnone, A., Bonaiuti, D., Focacci, A., Pacciani, R., Greco, A., and Spano, E., 2004. Parametric optimization of a high-lift turbine vane". ASME Paper No. GT 2004-54308.

[19] Sonoda, T., Arima, T., Olhofer, M., Sendhoff, B., Kost, F., and Giess, P., 2004. "A study of advanced high loaded transonic turbine airfoils". ASME Paper No. GT 2004-53773.

[20] Pini M., Turbomachinery Design Optimization using Adjoint Method and Accurate Equations of State, Dipartimento di Energia, Politechnico di Milano, December 2013

[21] S. Pierret, "Multi-objective and multi-disciplinary optimization of threedimensional turbomachinery blades," 6th World Congress of Structural and Multidisciplinary optimization, 2005.

[22] S. Pierret, R. F. Coelho, and H. Kato, "Multidisciplinary and multiple operating points shape optimization of three dimensional compressor blades," Journal of Structure and Multidisciplary optimization, 2007.

[23] Lepot, I., Mengistu, T., Hiernax, S. and Vriendt, O. D. 2011 Highly Loaded LPC Blade and Non Axisymmetric Hub Profiling Optimization For Enhanced Efficiency and Stability. In Proceedings of ASME Turbo Expo. Vancouver, Canada, GT2011-46261.

[24] Menter F. R., "Two-Equation Eddy-Viscosity Turbulence Models for Engineering Applications". AIAA Journal. 32(8). 1598–1605. August 1994.

[25] Menter F., R., Langtry R. B., Likki S. R., Suzen Y. B., Huang P. G., and Volker S.. "A Correlation-Based Transition Model Using Local Variables: Part I — Model Formulation", ASME-GT2004 53452 2004.

[26] Kapsoulis, D. H., Asouti, V, Kyriakos, G, Giannakoglou, C., Porziani S., Costa, E., Groth, C., Cella, U., and Biancolini, M., E., "Evolutionary Aerodynamics Shape Optimization Through the RBF4AERO Platform", ECCOMAS Congress 2016 VII European Congress on Computational Methods in Applied Sciences and Engineering, Crete Island, Greece, 5–10 June 2016